Journal of Applied and Computational Mechanics, Vol. 2, No. 4, (2016), 230-242
DOI: 10.22055/JACM.2016.12543

Journal of
Applied and Computational Mechanics

Uniaxial Buckling Analysis Comparison of Nanoplate and Nanocomposite Plate with Central Square Cut out Using Domain Decomposition Method

Majid Jamali[1,*], Taghi Shojaee[2], Bijan Mohammadi[4]

[1]School of Mechanical Engineering, Iran University of Science and Technology, Tehran, Iran, eng.mjamali@gmail.com
[2]School of Mechanical Engineering, Iran University of Science and Technology, Tehran, Iran, ta_shojaee@cmps2.iust.ac.ir
[3]Faculty of Mechanical Engineering, University of Kashan, Kashan, Iran, r.kolahchi@gmail.com
[4]School of Mechanical Engineering, Iran University of Science and Technology, Tehran, Iran, bijan_mohammadi@iust.ac.ir

Received November 11 2016; revised December 2 2016; accepted December 23 2016
Corresponding author: Majid Jamali, eng.mjamali@gmail.com

Abstract

A comparison of the buckling analysis of the nanoplate and nanocomposite plate with a central square hole embedded in the Winkler foundation is presented in this article. In order to enhance the mechanical properties of the nanoplate with a central cutout, the uniformly distributed carbon nanotubes (CNTs) are applied through the thickness direction. In order to define the shape function of the plate with a square cutout, the domain decomposition method and the orthogonal polynomials are used. At last, to obtain the critical buckling load of the system, the Rayleigh-Ritz energy method is provided. The impacts of the length and width of the plate, the dimension of the square cutout, and the elastic medium on the nanoplate and nanocomposite plate are presented in this study.

Keywords: Buckling analysis; Nanocomposite plate; Central square hole; Winkler foundation; Domain decomposition method; Rayleigh-Ritz energy method

1. Introduction

Nowadays, composite materials are applied as the modern generation materials in industry, and they are used instead of the conventional materials such as metallic, woody, and concrete materials. The development of the material science as well as the appearance of a novel branch of science which is called nanotechnology caused a modern group of composites entitled nanocomposites. The nanocomposites are a branch of composite materials whose reinforcing factor has a nanoscale. The marvelous discovery and invention of CNTs with extraordinary mechanical, thermal, electric, and magnetic properties tempted researchers to apply CNTs for reinforcing the composites. Some significant applications of the nanocomposites are abrasion resistant coatings, corrosion resistant coatings, conductive plastics, sensors, resistant lining in high temperature, and separation membranes for gases and petroleum fluids.

The buckling analysis of the nanoplates has been considered by many researchers hitherto. Murmu and Pradhan [1] investigated the elastic buckling behavior of the orthotropic small scale plates under biaxial compression. This study discussed the small-scale effects on the buckling loads of the nanoplates considering various materials and the geometrical parameters. The buckling of a single layer graphene sheet (SLGS) based on the nonlocal elasticity and the higher order shear deformation theory was addressed by Pradhan [2]. The levy type solution method for the vibration and buckling of the nanoplates using the nonlocal elasticity theory was reported by Aksencer and Aydogdu [3]. The results are presented for different nonlocal parameter, different length of plates, and different boundary conditions. In addition, the results demonstrated that nonlocality effects should be considered for the nanoscale plates. Hashemi and Samaei [4] carried out the buckling analysis of the nanoscale plates via the nonlocal elasticity theory. The effect of the length scale on the buckling behavior of a SLGS embedded in a Pasternak elastic medium using the nonlocal Mindlin plate theory was discussed by Samaei et al. [5]. It is understood that the nonlocal assumptions present larger buckling loads and stiffness of the elastic medium in comparison with the classical plate theory (CPT).

Farajpour et al. [6] reported the buckling analysis of variable thickness nanoplates using the nonlocal continuum mechanics. The result showed that the influence of the percentage change of the thickness on the stability of the graphene sheets is more remarkable in the strip-type nanoplates (nanoribbons) than in the square-type nanoplates. The buckling response of orthotropic SLGS is investigated using the nonlocal elasticity theory by Farajpour et al. [7]. The differential quadrature method (DQM) has been applied to solve the governing equations for various boundary conditions. It is explicit that the nonlocal effects play a considerable role in the stability behavior of the orthotropic nanoplates. Murmu et al. [8] addressed the nonlocal buckling of double-nanoplate-systems (DNPS) under biaxial compression. Both the synchronous and asynchronous buckling phenomenon of biaxially compressed DNPS are presented in this work. The buckling analysis of the double-orthotropic nanoplates embedded in the Pasternak elastic medium using the nonlocal elasticity theory was discussed by Radić et al. [9]. The effects of the small scale coefficient, the aspect ratio, and the stiffness of the internal elastic media and the external elastic foundation on the non-dimensional buckling was considered. Golmakania and Rezatalab [10] proposed the non-uniform biaxial buckling of the orthotropic nanoplates embedded in an elastic medium based on the nonlocal Mindlin plate theory. The influences of the small scale effect, the aspect ratio, the polymer matrix properties, the type of planar loading, the mode numbers, and the boundary conditions were probed in details.

CNTs can be used as an amplifier in different structure (beam, plate, etc.) and produce a nanocomposite system in order to enhance the mechanical properties and improve the behavior of the system. The buckling analysis of the laminated composite rectangular plates which were reinforced with CNTs using the analytical and finite element methods was carried out by Ghorbanpour Arani et al. [11]. In this article, the effects of the CNTs orientation angle, the edge conditions, and the aspect ratio on the critical buckling load are considered using both the analytical and finite element methods. The critical buckling load of the composite rectangle plate reinforced with CNTs which were subjected to an axial compressive load using CPT is discussed by Jam and Maghamikia [12]. Mohammadimehr et al. [13] proposed the buckling and vibration analysis of a double-bonded nanocomposite piezoelectric plate reinforced with a boron nitride nanotube based on the Eshelby-Mori-Tanaka approach using the modified couple stress theory under electro-thermo-mechanical loadings surrounded by an elastic foundation. The buckling analysis of the annular composite plates reinforced with CNTs which were subjected to the compressive and torsional loads was addressed by Asadi and Jam [14]. It is concluded that the stability of the plate increases as the thickness or the inner to outer ratio rises, and when CNTs are arranged in the circumferential direction, the highest buckling load is obtained. Mohammadimehr et al. [15] analyzed the biaxial buckling and bending of the smart nanocomposite plate reinforced with CNTs using the extended mixture rule approach.

Considering the literature, the buckling analysis of the nanoplate with a square cutout has not been studied yet. These considerations stimulated us to present the buckling analytical investigation of the nanoplate and nanocomposite plate with square cutout embedded by the Winkler medium. CPT is applied to simulate the plate, and the rule of mixture is used to obtain the mechanical properties of the nanocomposite plate. A detailed parametric study is conducted to explicate the effects of the dimensions of the plate, the length of the square cutout, and the elastic medium on the buckling analysis.

2. Nanocomposite Plate

Consider a nanocomposite plate as illustrated in Fig. 1, with the length a, width b, thickness h, and a central square hole with length d. The plate is subjected to an uniaxial load along x-direction (N_x) and surrounded by the Winkler foundation. Moreover, the plate is reinforced with CNTs through the thickness direction.

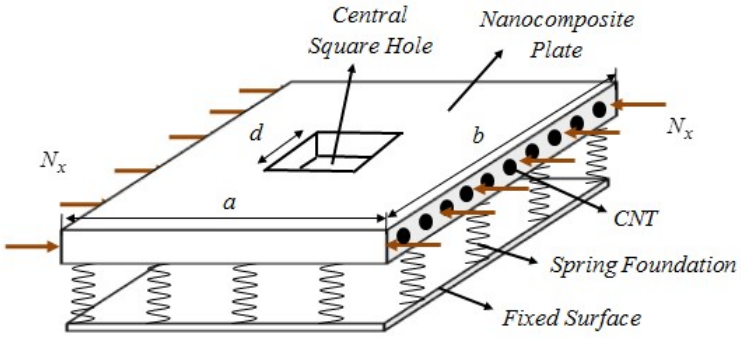

Fig. 1. A nanocomposite plate with a square cutout subjected to the uniaxial buckling load surrounded by the Winkler foundation.

The plate is assumed to be isotropic but after using the orthotropic CNTs in it, the system changes to the orthotropic structure. Therefore, by using CNTs in the plate, the mechanical properties of the system will be improved, thus, the effective mechanical properties of the nanocomposite plate are extended through the rule of mixture and the Young's modulus, E_{11} and E_{22}, and the shear modulus, G_{12}, are [16, 17]

$$E_{11} = \eta_1 V_{CNT} E_{11}^{CNT} + V_m E^m, \tag{1}$$

$$\frac{\eta_2}{E_{22}}=\frac{V_{CNT}}{E_{22}^{CNT}}+\frac{V_m}{E^m}, \tag{2}$$

$$\frac{\eta_3}{G_{12}}=\frac{V_{CNT}}{G_{12}^{CNT}}+\frac{V_m}{G^m}, \tag{3}$$

in which E_{11}^{CNT}, E_{22}^{CNT}, and G_{12}^{CNT} are the Young's modulus and the shear modulus of CNTs, respectively, moreover, E^m and G^m show the corresponding properties related to matrix. The CNT efficiency parameters, $\eta_j\ (j=1,2,3)$, demonstrate the scale-dependent material properties which are obtained by matching the effective mechanical properties of the nanocomposite plate calculated from the MD simulations with those calculated from the rule of mixture. The relation between the volume fractions of CNT, V_{CNT}, and the volume fractions of matrix, V_m, is expressed as:

$$V_{CNT}+V_m=1. \tag{4}$$

where for UD type

$$V_{CNT}=\frac{W_{CNT}}{W_{CNT}+\left(\frac{\rho_{CNT}}{\rho_m}\right)-\left(\frac{\rho_{CNT}}{\rho_m}\right)W_{CNT}}, \tag{5}$$

in which w_{CNT} expresses the mass fraction of the nanotube. The Poisson's ratio, υ_{12}, of the nanocomposite plate is:

$$\upsilon_{12}=V_{CNT}\upsilon_{12}^{CNT}+V_m\upsilon^m, \tag{6}$$

where υ_{12}^{CNT} and υ^m are the Poisson's ratios of CNTs and plate, respectively.

The constitutive equations of the nonlocal elasticity are:

$$\begin{Bmatrix}\sigma_{xx}\\ \sigma_{yy}\\ \sigma_{xy}\end{Bmatrix}=\begin{pmatrix}C_{11} & C_{12} & 0\\ C_{12} & C_{22} & 0\\ 0 & 0 & C_{66}\end{pmatrix}\begin{Bmatrix}\varepsilon_{xx}\\ \varepsilon_{yy}\\ \varepsilon_{xy}\end{Bmatrix}, \tag{7}$$

in which σ_{ij} and ε_{ij} are the stress and strain, respectively. C_{ij} are the elasticity coefficients with respect to the orthotropic structure and are considered as [18] :

$$C_{11}=\frac{E_{11}}{1-\upsilon_{12}\upsilon_{21}},C_{22}=\frac{E_{22}}{1-\upsilon_{12}\upsilon_{21}},C_{12}=\frac{\upsilon_{21}E_{11}}{1-\upsilon_{12}\upsilon_{21}},C_{66}=G_{12}. \tag{8}$$

3. Plate Theory

CPT is derived from the Euler–Bernoulli beam theory for thin plates. This theory is based on the following assumptions as:

- After displacement, straight lines normal to the mid-surface stay straight.
- After displacement, straight lines normal to the mid-surface stay normal.
- During displacement, thickness of the plate remains and does not change.

According to CPT, the displacement field can be considered as [19, 20]:

$$u(x,y,z)=z\beta_x\ , \tag{9}$$

$$v(x,y,z)=z\beta_y\ , \tag{10}$$

$$w=w(x,y), \tag{11}$$

where *u*, *v*, and *w* denote the displacement vector along x-, y-, and z-direction, respectively.

β_x and β_y are the rotations around x- and y-direction which are expressed as:

$$\beta_x=-\frac{\partial w}{\partial x}, \tag{12}$$

$$\beta_y=-\frac{\partial w}{\partial y}, \tag{13}$$

The von Karman strains based on the above displacement field can be calculated as:

$$\varepsilon_x = -z\frac{\partial^2}{\partial x^2}w\left(x,y\right), \tag{14}$$

$$\varepsilon_y = -z\frac{\partial^2}{\partial y^2}w\left(x,y\right), \tag{15}$$

$$\gamma_{xy} = -2z\frac{\partial^2}{\partial x\,\partial y}w\left(x,y\right), \tag{16}$$

where ε_x , ε_y , and γ_{xy} are the normal strain along x and y axis and the shear strain component, respectively.

4. Nonlocal Elasticity Theory and Energy Method

In nanoscale the local theory is not valid, and some other theories are suggested such as the Eringen's nonlocal elasticity theory. This theory expresses that the stress state at a reference point in the body is related not only to the strain state at this point but to the strain states at all of the points throughout the body. According to this theory, it can be express as [21]:

$$\left(1-\mu^2\nabla^2\right)\sigma_{ij}^{nl} = \sigma_{ij}^{l}, \tag{17}$$

where the parameter $\mu=\left(e_0a\right)^2$ demonstrates the small scale effect regarding the nanoscale, and ∇^2 is the Laplacian operator. It should be represented that the nonlocal stresses tensor changes to a local one when the nonlocal parameter is set to zero.

The energy method is applied to obtain the equations of the system as [22]:

$$\Pi = U - W\ , \tag{18}$$

where *U* and *W* are the strain energy and external works, respectively, and Π is the total energy of the system.

4.1. Strain energy

The strain energy can be obtained as [23]:

$$U = \frac{1}{2}\int_A\int_{\frac{-h}{2}}^{\frac{h}{2}}\left(\sigma_{xx}\varepsilon_{xx}+\sigma_{yy}\varepsilon_{yy}+\sigma_{xy}\gamma_{xy}\right)dz\,dA\,. \tag{19}$$

By substituting Eqs. (14-16) and Eq. (7) into Eq. (19) we obtain:

$$U = \frac{1}{2}\int_A\left(-M_x\frac{\partial^2}{\partial x^2}w\left(x,y\right)-2M_{xy}\frac{\partial^2}{\partial y\,\partial x}w\left(x,y\right)-M_y\frac{\partial^2}{\partial y^2}w\left(x,y\right)\right)dA \tag{20}$$

in which the moment resultants are considered as [24]:

$$\left(M_x,M_y,M_{xy}\right) = \int_{\frac{-h}{2}}^{\frac{h}{2}}\left(\sigma_x,\sigma_y,\sigma_{xy}\right)z\,dz\,, \tag{21}$$

4.2. External works

According to Fig. 1, the nanocomposite plate is subjected to two types of forces such as the foundation forces and the buckling load.

4.2.1. Foundation forces

The plate is embedded by the Winkler foundation. As it is known, this foundation model considers the normal load from the environment to the system. Therefore, the work of this foundation can be obtained as [25]:

$$W_e = -\int_A\left(K_w w\right)w\,dA\,, \tag{22}$$

K_w is the Winkler's spring modulus.

4.2.2. Buckling load

The nanocomposite plate is subjected to buckling, thus the work of this force can be calculated as [22]:

$$W_b = -\frac{1}{2}\int_A\left(N_{xx}\left(\frac{\partial}{\partial x}w\left(x,y\right)\right)^2+N_{yy}\left(\frac{\partial}{\partial y}w\left(x,y\right)\right)^2\right)dA\,, \tag{23}$$

the buckling load is uniaxial, so $N_{xx}=-P$ and $N_{yy}=0$.

With respect to the Eringen's nonlocal elasticity theory and the energy method, the total energy of the nanocomposite plate is equal to:

$$\Pi = \int_A \left(\mu^2 P \left(\frac{\partial^2 w}{\partial x^2} \right)^2 + \mu^2 P \left(\frac{\partial^2 w}{\partial y \partial x} \right)^2 - \frac{1}{2} P \left(\frac{\partial w}{\partial x} \right)^2 + \mu^2 P \left(\frac{\partial w}{\partial x} \right) \left(\frac{\partial^3 w}{\partial x^3} \right) + \mu^2 P \left(\frac{\partial w}{\partial x} \right) \left(\frac{\partial^3 w}{\partial y^2 \partial x} \right) \right.$$
$$-2\mu^2 K_w w \left(\frac{\partial^2 w}{\partial x^2} \right) - 2\mu^2 K_w w \left(\frac{\partial^2 w}{\partial y^2} \right) - 2\mu^2 K_w \left(\frac{\partial w}{\partial y} \right)^2 + K_w w^2 - 2\mu^2 K_w \left(\frac{\partial w}{\partial x} \right)^2 \tag{24}$$
$$\left. -\frac{1}{2} M_x \left(\frac{\partial^2 w}{\partial x^2} \right) - M_{xy} \left(\frac{\partial^2 w}{\partial y \partial x} \right) - \frac{1}{2} M_y \left(\frac{\partial^2 w}{\partial y^2} \right) \right) dA ,$$

where

$$M_x = -D11 \left(\frac{\partial^2}{\partial x^2} w(x,y) \right) h - D12 \left(\frac{\partial^2}{\partial y^2} w(x,y) \right) h , \tag{25}$$

$$M_y = -D_{12} \left(\frac{\partial^2}{\partial x^2} w(x,y) \right) h - D_{22} \left(\frac{\partial^2}{\partial y^2} w(x,y) \right) h , \tag{26}$$

$$M_{xy} = -2 D_{66} \left(\frac{\partial^2}{\partial y \partial x} w(x,y) \right) h , \tag{27}$$

and the stiffness components in aforementioned equations can be specified as [16]:

$$(D_{11}, D_{22}, D_{12}, D_{66},) = \int_{-\frac{h}{2}}^{\frac{h}{2}} z^2 . (C_{11}(z), C_{22}(z), C_{12}(z), C_{66}(z)) dz , \tag{28}$$

5. Buckling of Nanocomposite Plate with Cutout

5.1. Domain decomposition method and orthogonal polynomials

In this section, the shape function of the plate with a central cutout in the simply supported boundary conditions (S-S-S-S) will be calculated by applying the domain decomposition method and the orthogonal polynomials. At first, the domain decomposition method [22, 26-33], which considers not only the outer boundary conditions (S-S-S-S) but the inner (cut out edges) free boundary condition, is used to divide the plate to some subdomains. Because of the two symmetrical conditions, only one quarter of the rectangular plate with a central square cutout needs to be considered as Fig. 2; therefore, one fourth of the plate is divided to three subdomains.

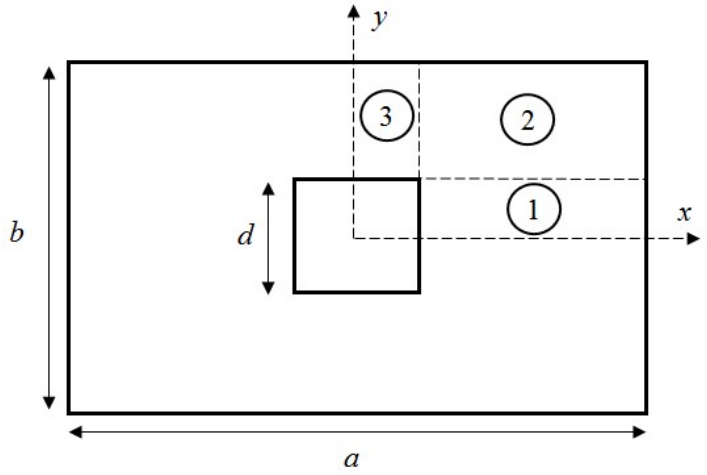

Fig. 2. Illustration of dividing the nanocomposite plate with a cutout to three sub-domains.

After partitioning the nanocomposite plate with a central square cutout, the shape function should be determined. The orthogonal polynomials [31] are applied to present the shape function of each subdomain considering the geometric boundary conditions. The deflection shape functions for each subdomain can be defined as:

$$w^{(1)}(x,y) = \sum_{m=1}^{M} \sum_{n=1}^{N} A_{mn}^{(1)} f_m^{(1)}(x) g_n^{(1)}(y), \tag{29}$$

$$w^{(2)}(x,y) = \sum_{m=1}^{M} \sum_{n=1}^{N} A_{mn}^{(2)} f_m^{(2)}(x) g_n^{(2)}(y), \tag{30}$$

$$w^{(3)}(x,y)=\sum_{m=1}^{M}\sum_{n=1}^{N}A_{mn}^{(3)}f_m^{(3)}(x)g_n^{(3)}(y), \tag{31}$$

where, the superscripts (1), (2), and (3) imply the subdomain 1, 2, and 3, respectively. $w^{(i)}(i=1,2,3)$ are the shape functions of the subdomain 1, 2, and 3, respectively. $A_{mn}^{(i)}$ are the undetermined coefficients of the shape functions $w^{(i)}$. $f_m^{(i)}(x)$ are the polynomial functions which consider the essential boundary conditions along x-direction, while $g_n^{(i)}(y)$ are the polynomial functions which consider the essential boundary conditions along y-direction. The orthogonal polynomial functions $f_m^{(i)}(x)$ and $g_n^{(i)}(y)$ are made by the Gram–Schmidt process [31]. The initial polynomials $(f_1(x), g_0(x))$ which initially satisfy the essential boundary conditions can be calculated for different boundary conditions according to Table 1. The process is as [31]:

$$f_2(x)=(g_0(x)-A_1)f_1(x), \tag{32}$$

$$f_{k+1}(x)=(g_0(x)-A_k)f_k(x)-B_k f_{k-1}(x),\ k\geq 2 \tag{33}$$

where

$$A_k=\frac{\int_0^1 g_0(x)f_k(x)f_k(x)dx}{\int_0^1 f_k(x)f_k(x)dx}, \tag{34}$$

$$B_k=\frac{\int_0^1 g_0(x)f_k(x)f_{k-1}(x)dx}{\int_0^1 f_{k-1}(x)f_{k-1}(x)dx}. \tag{35}$$

In order to specify the functions $g_n(y)$, the same process of determining $f_m(x)$ as defined in Eqs. (32-35) can be used.

Therefore, the shape functions of three subdomains were defined hitherto, and the final step to calculate the buckling load is to determine the deflection functions of three subdomains in terms of the undetermined coefficients of one of the subdomains. Thus, the best way is to apply some spots.

Table 1. Starting polynomials for sets of the orthogonal polynomials [22].

Boundary Conditions	Starting Polynomials, $f_1(x)$	Generating Functions, $g_0(x)$
Free-Free $f_1''(0)=f_1'''(0)=0,$ $f_1''(1)=f_1'''(1)=0$	1.0	x
Free-Simply supported $f_1''(0)=f_1'''(0)=0,$ $f_1(1)=f_1''(1)=0$	$1-x$	x^2-2x
Free-Clamped $f_1''(0)=f_1'''(0)=0,$ $f_1(1)=f_1'(1)=0$	$3-4x+x^4$	x
Symmetric-Free $f_1'(0)=f_1'''(0)=0,$ $f_1''(1)=f_1'''(1)=0$	$1+x^2$	$1+x^2$
Symmetric- Simply supported $f_1'(0)=f_1'''(0)=0,$ $f_1(1)=f_1''(1)=0$	$5-6x^2+x^4$	x^2
Symmetric- Clamped		

$f_1'(0)=f_1'''(0)=0,$ $f_1(1)=f_1'(1)=0$	$1-2x^2+x^4$	$1-x^2$
Anti-symmetric- Simply supported		
$f_1(0)=f_1''(0)=0,$ $f_1(1)=f_1''(1)=0$	$x-2x^3+x^4$	x^2

According to the mathematical derivation, in the interconnecting boundary between the subdomains the undetermined coefficients of subdomains 1, 2, and 3 are related together [30-33].

5.2. Rayleigh-Ritz method

The Rayleigh-Ritz method is used to calculate the buckling load of the nanocomposite plate with a central square cutout. As noted before, because of two symmetrical conditions, only one quarter of the rectangular plate with a central square cutout needs to be considered. The total energy of the plate with the cutout is determined as:

$$\Pi = \Pi^{(1)} + \Pi^{(2)} + \Pi^{(3)}, \tag{36}$$

$\Pi^{(i)}\,(i=1,2,3)$ are the total energy of the subdomains 1, 2, and 3, respectively which are defined with respect to Eq. (24) and Fig. 2 as:

$$\begin{aligned}\Pi^{(1)} = \int_0^{\frac{d}{2}}\int_{\frac{d}{2}}^{\frac{a}{2}}\Bigg(&\mu^2 P\left(\frac{\partial^2 w^{(1)}}{\partial x^2}\right)^2+\mu^2 P\left(\frac{\partial^2 w^{(1)}}{\partial y\,\partial x}\right)^2-\frac{1}{2}P\left(\frac{\partial w^{(1)}}{\partial x}\right)^2+\mu^2 P\left(\frac{\partial w^{(1)}}{\partial x}\right)\left(\frac{\partial^3 w^{(1)}}{\partial x^3}\right)+\mu^2 P\left(\frac{\partial w^{(1)}}{\partial x}\right)\left(\frac{\partial^3 w^{(1)}}{\partial y^2\,\partial x}\right)\\&-2\mu^2 K_w w^{(1)}\left(\frac{\partial^2 w^{(1)}}{\partial x^2}\right)-2\mu^2 K_w w^{(1)}\left(\frac{\partial^2 w^{(1)}}{\partial y^2}\right)-2\mu^2 K_w\left(\frac{\partial w^{(1)}}{\partial y}\right)^2+K_w\left(w^{(1)}\right)^2-2\mu^2 K_w\left(\frac{\partial w^{(1)}}{\partial x}\right)^2\\&-\frac{1}{2}M_x\left(\frac{\partial^2 w^{(1)}}{\partial x^2}\right)-M_{xy}\left(\frac{\partial^2 w^{(1)}}{\partial y\,\partial x}\right)-\frac{1}{2}M_y\left(\frac{\partial^2 w^{(1)}}{\partial y^2}\right)\Bigg)dx\,dy,\end{aligned} \tag{37}$$

$$\begin{aligned}\Pi^{(2)} = \int_{\frac{d}{2}}^{\frac{b}{2}}\int_{\frac{d}{2}}^{\frac{a}{2}}\Bigg(&\mu^2 P\left(\frac{\partial^2 w^{(2)}}{\partial x^2}\right)^2+\mu^2 P\left(\frac{\partial^2 w^{(2)}}{\partial y\,\partial x}\right)^2-\frac{1}{2}P\left(\frac{\partial w^{(2)}}{\partial x}\right)^2+\mu^2 P\left(\frac{\partial w^{(2)}}{\partial x}\right)\left(\frac{\partial^3 w^{(2)}}{\partial x^3}\right)+\mu^2 P\left(\frac{\partial w^{(2)}}{\partial x}\right)\left(\frac{\partial^3 w^{(2)}}{\partial y^2\,\partial x}\right)\\&-2\mu^2 K_w w^{(2)}\left(\frac{\partial^2 w^{(2)}}{\partial x^2}\right)-2\mu^2 K_w w^{(2)}\left(\frac{\partial^2 w^{(2)}}{\partial y^2}\right)-2\mu^2 K_w\left(\frac{\partial w^{(2)}}{\partial y}\right)^2+K_w\left(w^{(2)}\right)^2-2\mu^2 K_w\left(\frac{\partial w^{(2)}}{\partial x}\right)^2\\&-\frac{1}{2}M_x\left(\frac{\partial^2 w^{(2)}}{\partial x^2}\right)-M_{xy}\left(\frac{\partial^2 w^{(2)}}{\partial y\,\partial x}\right)-\frac{1}{2}M_y\left(\frac{\partial^2 w^{(2)}}{\partial y^2}\right)\Bigg)dx\,dy,\end{aligned} \tag{38}$$

$$\begin{aligned}\Pi^{(3)} = \int_{\frac{d}{2}}^{\frac{b}{2}}\int_0^{\frac{d}{2}}\Bigg(&\mu^2 P\left(\frac{\partial^2 w^{(3)}}{\partial x^2}\right)^2+\mu^2 P\left(\frac{\partial^2 w^{(3)}}{\partial y\,\partial x}\right)^2-\frac{1}{2}P\left(\frac{\partial w^{(3)}}{\partial x}\right)^2+\mu^2 P\left(\frac{\partial w^{(3)}}{\partial x}\right)\left(\frac{\partial^3 w^{(3)}}{\partial x^3}\right)+\mu^2 P\left(\frac{\partial w^{(3)}}{\partial x}\right)\left(\frac{\partial^3 w^{(3)}}{\partial y^2\,\partial x}\right)\\&-2\mu^2 K_w w^{(3)}\left(\frac{\partial^2 w^{(3)}}{\partial x^2}\right)-2\mu^2 K_w w^{(3)}\left(\frac{\partial^2 w^{(3)}}{\partial y^2}\right)-2\mu^2 K_w\left(\frac{\partial w^{(3)}}{\partial y}\right)^2+K_w\left(w^{(3)}\right)^2-2\mu^2 K_w\left(\frac{\partial w^{(3)}}{\partial x}\right)^2\\&-\frac{1}{2}M_x\left(\frac{\partial^2 w^{(3)}}{\partial x^2}\right)-M_{xy}\left(\frac{\partial^2 w^{(3)}}{\partial y\,\partial x}\right)-\frac{1}{2}M_y\left(\frac{\partial^2 w^{(3)}}{\partial y^2}\right)\Bigg)dx\,dy,\end{aligned} \tag{39}$$

Therefore, the total energy of the plate with the cutout is specified in terms of the undetermined coefficients of the shape function of the subdomain 1. The critical buckling load of the plate with the cutout after applying the Rayleigh-Ritz method is determined by putting the coefficient determinant of the equations equal to zero.

6. Results

The results of the buckling analysis associated with the nanoplate and nanocomposite plate with a central square cutout surrounded by the Winkler foundation are provided in this section. The goal of this essay is to consider the effects of the dimensions of the plate, the length of the square cutout, and the elastic medium on the critical buckling load of the plate. Here, the Poly-co-vinylene, referred to as PmPV, and the orthotropic CNTs are selected as the matrix and the reinforcement materials, respectively. The material properties of CNTs and PmPV are addressed in Table 2 [34].

Table 2. Material properties of the matrix and CNTs [34].

Matrix	CNTs
$E^m = 2.1(GPa)$	$E_{11}^{CNT} = 5.6466(TPa)$
$\upsilon_m = 0.34$	$E_{22}^{CNT} = 7.08(TPa)$
	$G_{12}^{CNT} = 1.9447(TPa)$
	$\upsilon_{12}^{CNT} = 0.175$

Table 3 provides the buckling load for different values of the nonlocal parameter and the aspect ratio of the length to the thickness. As can be seen, the present results match closely with those defined by Hashemi and Samaei [4], Pradhan and Murmu [35], and Pradhan [2].

In this editorial, the buckling load ratio and the dimensionless Winkler modulus are determined as: ($Buckling\ load\ ratio = \frac{Buckling\ load\ from\ nonlocal\ theory\ (P_{nl})}{Buckling\ load\ from\ local\ theory\ (P_l)}$) and ($K_W = \frac{K_w\ h}{E^m}$), respectively.

Fig. 3 shows the effect of CNTs in the plate on the buckling load ratio with respect to the nonlocal parameter. It is obvious that the Isotropic type (plate without CNTs) has the minimum effect on the critical buckling load ratio in comparison with the Composite type in which CNTs are as amplifier in the plate. However, it can be comprehended that CNTs can enhance the mechanical properties of the plate, and as a result, the critical buckling load ratio increases.

Table 3. A comparison between the buckling analysis of SLGS using the theories of the classical plate, the higher order shear deformation, and the Mindlin plate.

a/h	e_0a	CPT [35]	higher order plate theory [2]	Mindlin plate theory [4]	present
100	0.0	9.8791	9.8671	9.8671	9.8790
	0.5	9.4156	9.4031	9.4029	9.4156
	1.0	8.9947	8.9807	8.9803	8.9945
	1.5	8.6073	8.5947	8.5939	8.6073
	2.	8.2537	8.2405	8.2393	8.2533
20	0.0	9.8177	9.8067	9.8067	9.8172
	0.5	9.3570	9.3455	9.3455	9.3570
	1.0	8.9652	8.9528	8.9527	8.9648
	1.5	8.5546	8.5420	8.5420	8.5546
	2.0	8.2114	8.1900	8.1898	8.2111

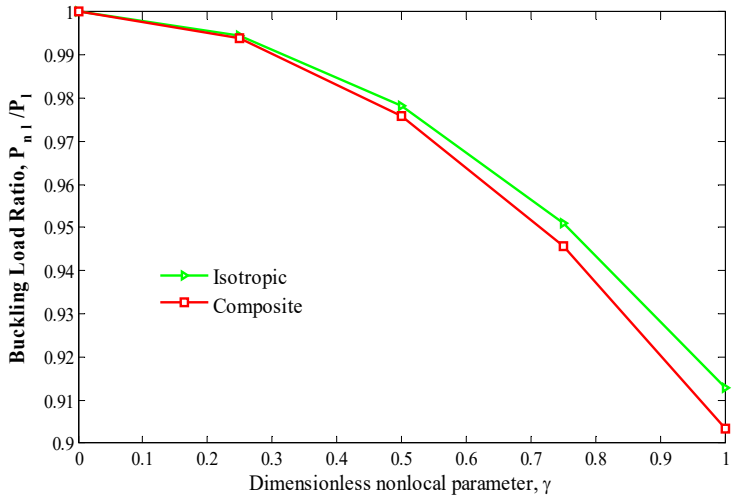

Fig. 3. A comparison between the Isotropic and Composite types on the buckling load ratio versus the dimensionless nonlocal parameter.

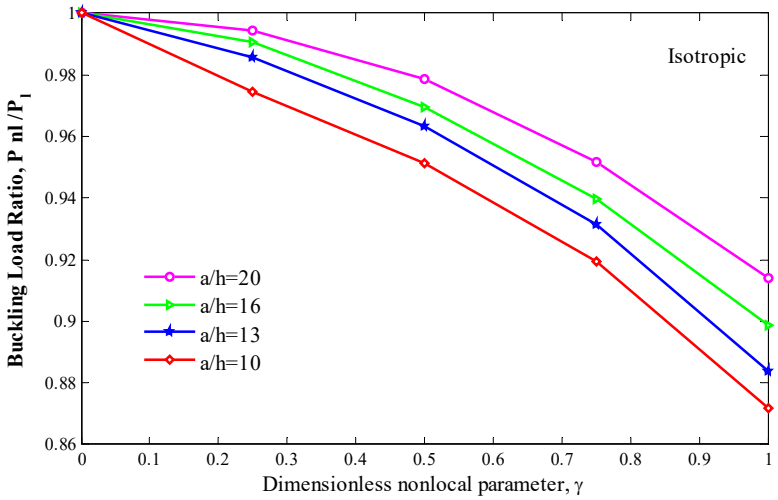

Fig. 4a

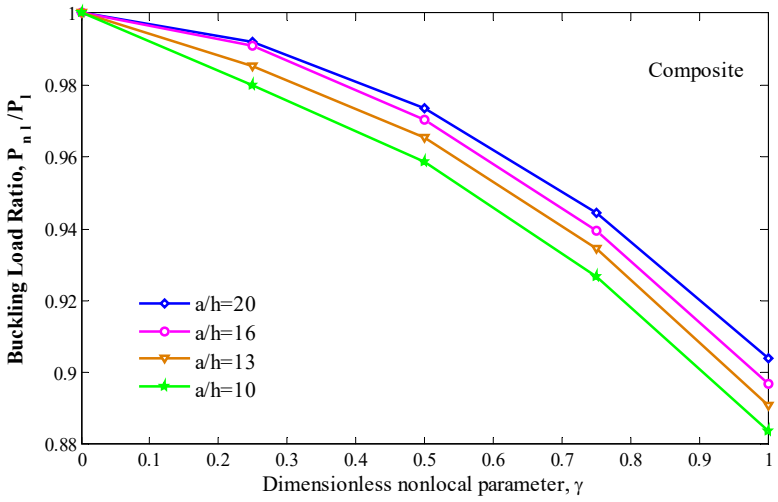

Fig. 4b

Fig. 4. Effect of the length of the plate on the critical buckling load ratio in terms of the dimensionless nonlocal parameter.

Fig. 4 illustrates the effect of the length of the plate on the buckling load ratio by considering the dimensionless nonlocal parameter. As can be seen, by increasing the nonlocal parameter, the critical buckling load ratio decreases. The figure shows that an increase in the length causes more buckling load ratio, because by increasing the length, the stiffness of the system decreases so the critical buckling load decreases, too, but variation of the local buckling load is more than the nonlocal buckling load; therefore, the critical buckling load ratio increases. It is apparent that the effect of the length on the buckling load ratio is more remarkable in the high value of the nonlocal parameter.

The variation of the critical buckling load ratio in terms of the nonlocal parameter is analyzed with respect to different aspect ratios of the nanocomposite plate with the square cutout in Fig. 5. It is obvious that the effectiveness order of the aspect ratio on the buckling load ratio from high to low is as $a/b\rangle 1$, $a/b=1$, and $a/b\langle 1$, respectively. To understand the reason of this order, it is better to look at Fig. 1 and consider the length and width of the plate and the direction of the uniaxial buckling load. Moreover, considering the figure, the buckling load ratio decreases by increasing the nonlocal parameter.

The effect of the elastic medium on the critical buckling ratio is examined in this section. Fig. 7 analyzes the variation of the buckling load ratio considering the nonlocal parameter and different magnitude of the Winkler modulus parameter (K_W). It is obvious that the Winkler modulus parameter improves the buckling behavior of the plate because the Winkler foundation imposes a normal force on the system; therefore, these foundations increase the stiffness of the system and the buckling load ratio.

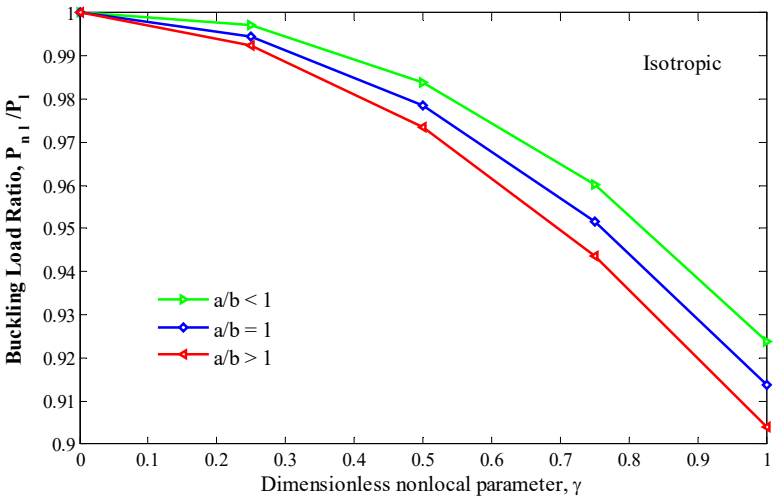

Fig. 5a

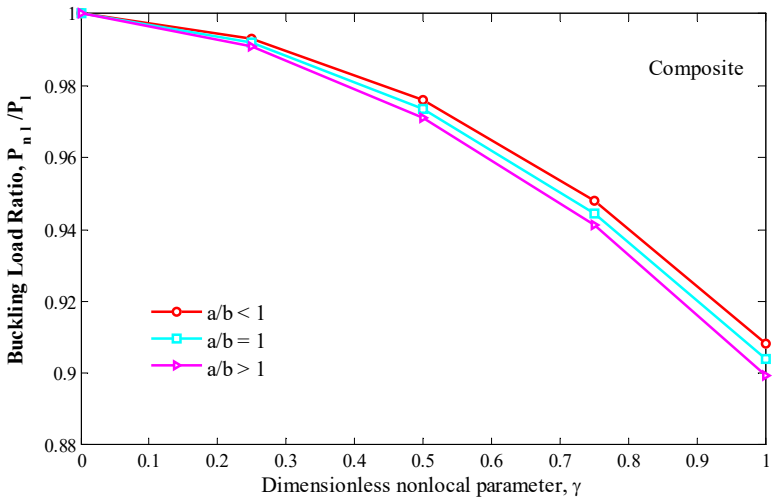

Fig. 5a

Fig. 5. Effect of the aspect ratio of the plate on the buckling load ratio versus the dimensionless nonlocal parameter.

Fig. 6 considers the effect of the length of the square cutout in the nanocomposite plate on the buckling load ratio in terms of the nonlocal parameter. It is apparent that the existence of a hole in the plate causes a defect in the system and weakens the buckling behavior; therefore, by increasing the length of the square cutout in the plate the buckling load ratio increases. In addition, the effect of the length of the hole on the critical buckling load ratio is more considerable for high dimensionless nonlocal parameter.

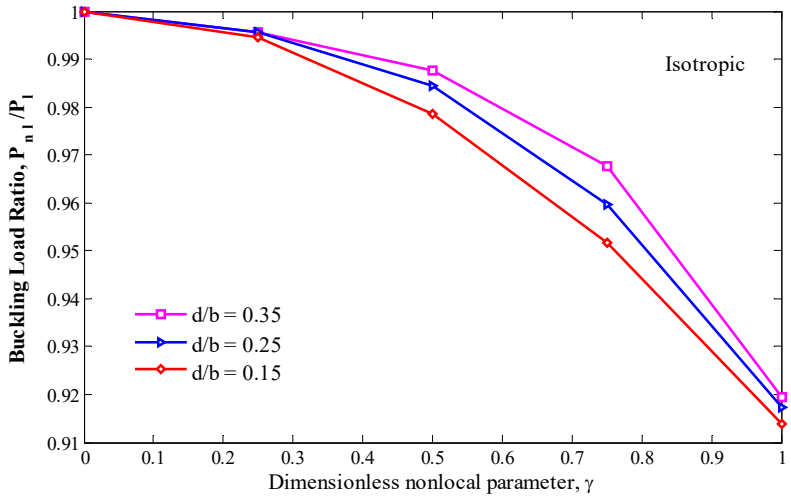

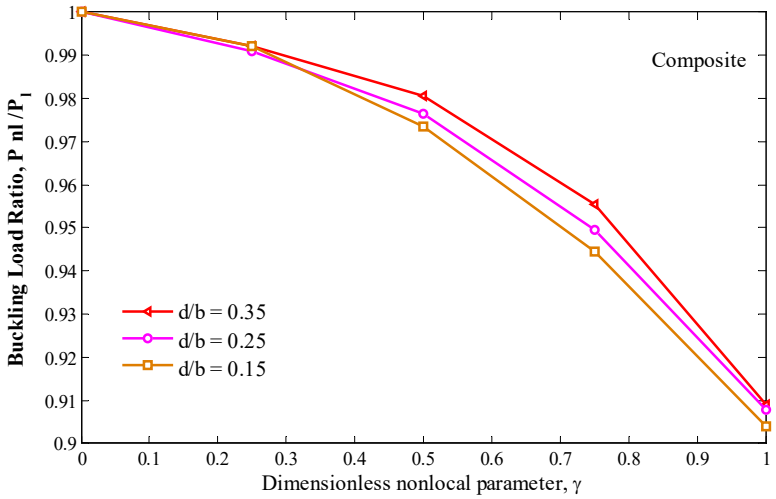

Fig. 6a

Fig. 6. Variation of the critical buckling load ratio by considering dimensionless nonlocal parameter for different length of the square cutout in the plate.

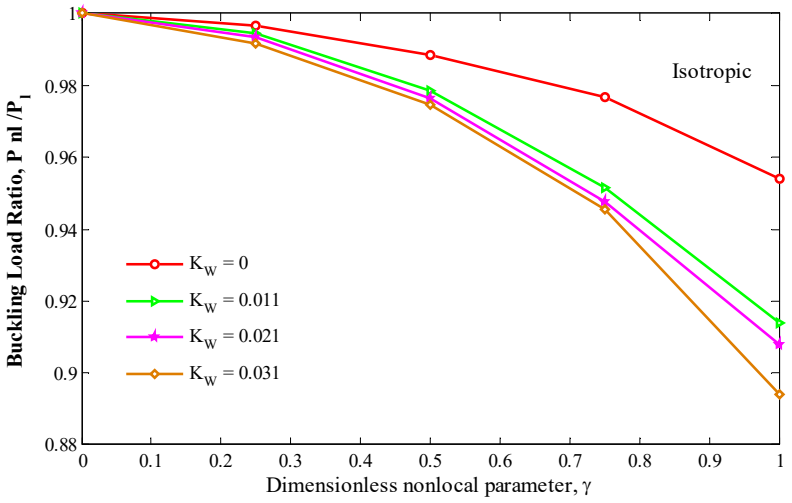

Fig. 7a

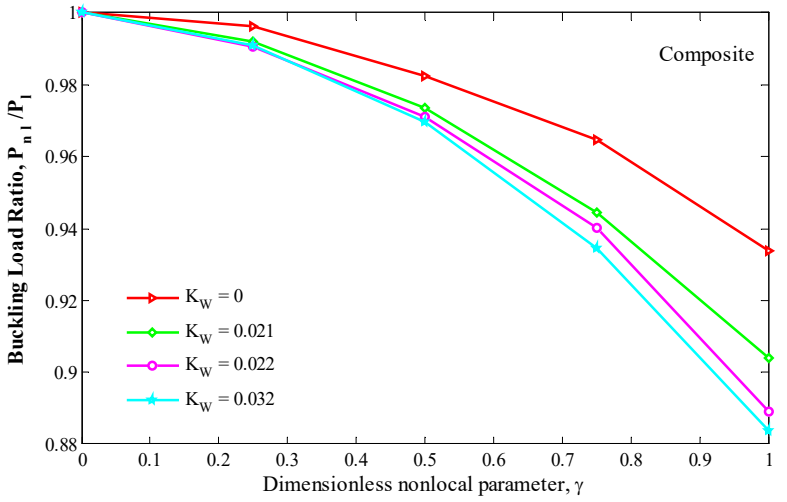

Fig. 7b

Fig. 7. Buckling load ratio versus dimensionless nonlocal parameter for different values of the Winkler modulus parameter.

7. Conclusion

The buckling load ratio of the nanoplate and nanocomposite plate with a square cutout reinforced with CNTs which were subjected to uniaxial buckling load was investigated in this article. The plate was surrounded by the Winkler foundation, and the Eringen's nonlocal elasticity theory was used to consider the nanoscale effect. In order to define the shape function of the plate with the cutout, the domain decomposition method and the orthogonal polynomials were applied. Finally, the Rayleigh-Ritz energy method was used to obtain the critical buckling load of the system so that the impacts of the dimensions of the plate, the length of the square cutout, and the elastic medium on the critical buckling load of the nanoplate and nanocomposite plate were distinguished. The results indicated that applying CNT as amplifier in the plate increased the properties of the system. In addition, by increasing the dimensions of the plate, the buckling load ratio of the plate with the square cutout increased as well. Moreover, existence of a hole in the plate caused a defect in the system and weakened the buckling behavior; therefore, by increasing the length of the square cutout in the plate, the buckling load ratio increased. Furthermore, utilizing the Winkler modulus parameter improved the buckling behavior of the plate.

References

[1] Murmu, T., and Pradhan, S. C., "Buckling of biaxially compressed orthotropic plates at small scales," Mechanics Research Communications, Vol. 36, pp. 933-938, 2009.

[2] Pradhan, S. C., "Buckling of single layer graphene sheet based on nonlocal elasticity and higher order shear deformation theory," Physics Letters A, Vol. 373, pp. 4182-4188, 2009.

[3] Aksencer, T., and Aydogdu, M., "Levy type solution method for vibration and buckling of nanoplates using nonlocal elasticity theory," Physica E: Low-dimensional Systems and Nanostructures, Vol. 43, pp. 954-959, 2011.

[4] Hashemi, S. H., and Samaei, A. T., "Buckling analysis of micro/nanoscale plates via nonlocal elasticity theory," Physica E: Low-dimensional Systems and Nanostructures, Vol. 43, pp. 1400-1404, 2011.

[5] Samaei, A. T., Abbasion, S., and Mirsayar, M. M., "Buckling analysis of a single-layer graphene sheet embedded in an elastic medium based on nonlocal Mindlin plate theory," Mechanics Research Communications, Vol. 38, pp. 481-485, 2011.

[6] Farajpour, A., Danesh, M., and M. Mohammadi, "Buckling analysis of variable thickness nanoplates using nonlocal continuum mechanics," Physica E: Low-dimensional Systems and Nanostructures, Vol. 44, pp. 719-727, 2011.

[7] Farajpour, A., Shahidi, A. R., Mohammadi, M., and Mahzoon, M., "Buckling of orthotropic micro/nanoscale plates under linearly varying in-plane load via nonlocal continuum mechanics," Composite Structures, Vol. 94, pp. 1605-1615, 2012.

[8] Murmu, T., Sienz, J., Adhikari, S., and Arnold, C., "Nonlocal buckling of double-nanoplate-systems under biaxial compression," Composites Part B: Engineering, Vol. 44, pp. 84-94, 2013.

[9] Radić, N., Jeremić, D., Trifković, S., and Milutinović, M., "Buckling analysis of double-orthotropic nanoplates embedded in Pasternak elastic medium using nonlocal elasticity theory," Composites Part B: Engineering, Vol. 61, pp. 162-171, 2014.

[10] Golmakani, M. E., and Rezatalab, J., "Nonuniform biaxial buckling of orthotropic nanoplates embedded in an elastic medium based on nonlocal Mindlin plate theory," Composite Structures, Vol. 119, pp. 238-250, 2015.

[11] Arani, A. G., Maghamikia, S., Mohammadimehr, M., and Arefmanesh, A., "Buckling analysis of laminated composite rectangular plates reinforced by SWCNTs using analytical and finite element methods," Journal of Mechanical Science and Technology, Vol. 25, pp. 809-820, 2011.

[12] Jam, J. E., and Maghamikia, S., "Elastic buckling of composite plate reinforced with carbon nano tubes," International Journal of Engineering Science and Technology, Vol. 3, pp. 4090-4101, 2011.

[13] Mohammadimehr, M., Mohandes, M., and Moradi, M., "Size dependent effect on the buckling and vibration analysis of double-bonded nanocomposite piezoelectric plate reinforced by boron nitride nanotube based on modified couple stress theory," Journal of Vibration and Control, 2014.

[14] Asadi, E., and Jam, J. E., "Analytical and Numerical Buckling Analysis of Carbon Nanotube Reinforced Annular Composite Plates," Int J Advanced Design and Manufacturing Technology, Vol. 7, pp. 35-44, 2014.

[15] Mohammadimehr, M., Rousta-Navi, B., and Ghorbanpour-Arani, A., "Biaxial Buckling and Bending of Smart Nanocomposite Plate Reinforced by CNTs using Extended Mixture Rule Approach," Mechanics of Advanced Composite Structures, Vol. 1, pp. 17-26, 2014.

[16] Ghorbanpour Arani, A., Jamali, M., Mosayyebi, M., and Kolahchi, R., "Wave propagation in FG-CNT-reinforced piezoelectric composite micro plates using viscoelastic quasi-3D sinusoidal shear deformation theory," Composites Part B: Engineering, Vol. 95, pp. 209-224, 2016.

[17] Ghorbanpour Arani, A., Jamali, M., Ghorbanpour-Arani, A., Kolahchi, R., and Mosayyebi, M., "Electro-magneto wave propagation analysis of viscoelastic sandwich nanoplates considering surface effects," Proceedings of the Institution of Mechanical Engineers, Part C: Journal of Mechanical Engineering Science,

2016.
[18] Wattanasakulpong, N., and Chaikittiratana, A., "Exact solutions for static and dynamic analyses of carbon nanotube-reinforced composite plates with Pasternak elastic foundation," Applied Mathematical Modelling, Vol. 39, pp. 5459-5472, 2015.
[19] Ashoori Movassagh, A., and Mahmoodi, M. J., "A micro-scale modeling of Kirchhoff plate based on modified strain-gradient elasticity theory," European Journal of Mechanics - A/Solids, Vol. 40, pp. 50-59, 2013.
[20] Ghorbanpour Arani, A., and Shokravi, M., "Vibration response of visco-elastically coupled double-layered visco-elastic graphene sheet systems subjected to magnetic field via strain gradient theory considering surface stress effects," Proceedings of the Institution of Mechanical Engineers, Part N: Journal of Nanoengineering and Nanosystems, 2014.
[21] Ghorbanpour Arani, A., Jamali, M., Mosayyebi, M., and Kolahchi, R., "Analytical modeling of wave propagation in viscoelastic functionally graded carbon nanotubes reinforced piezoelectric microplate under electro-magnetic field," Proceedings of the Institution of Mechanical Engineers, Part N: Journal of Nanoengineering and Nanosystems, 2015.
[22] Pan, Z., Cheng, Y., and Liu, J., "A semi-analytical analysis of the elastic buckling of cracked thin plates under axial compression using actual non-uniform stress distribution," Thin-Walled Structures, Vol. 73, pp. 229-241, 2013.
[23] Ghorbanpour Arani, A., Kolahchi, R., Mosayyebi, M., and Jamali, M., "Pulsating fluid induced dynamic instability of visco-double-walled carbon nano-tubes based on sinusoidal strain gradient theory using DQM and Bolotin method," International Journal of Mechanics and Materials in Design, pp. 1-22, 2014.
[24] Reddy, J. N., "Mechanics of Laminated Composite Plates and Shells: Theory and Analysis," second edition ed: CRC Press, 2003.
[25] Ghorbanpour Arani, A., Kolahchi, R., and Vossough, H., "Buckling analysis and smart control of SLGS using elastically coupled PVDF nanoplate based on the nonlocal Mindlin plate theory," Physica B: Condensed Matter, Vol. 407, pp. 4458-4465, 2012.
[26] Lam, K. Y., Hung, K. C., and Chow, S. T., "Vibration analysis of plates with cutouts by the modified Rayleigh-Ritz method," Applied Acoustics, Vol. 28, pp. 49-60, 1989.
[27] Lam K. Y., and Hung, K. C., "Orthogonal polynomials and sub-sectioning method for vibration of plates," Computers & Structures, Vol. 34, pp. 827-834, 1990.
[28] Liew, K. M., Hung, K. C., and Lim, M. K., "Method of domain decomposition in vibrations of mixed edge anisotropic plates," International Journal of Solids and Structures, Vol. 30, pp. 3281-3301, 1993.
[29] Liew, K. M., Hung, K. C., and Sum, Y. K., "Flexural vibration of polygonal plates: treatments of sharp re-entrant corners," Journal of Sound and Vibration, Vol. 183, pp. 221-238, 1995.
[30] Liew, K. M., Kitipornchai, S., Leung, A. Y. T., and Lim, C. W., "Analysis of the free vibration of rectangular plates with central cut-outs using the discrete Ritz method," International Journal of Mechanical Sciences, Vol. 45, pp. 941-959, 2003.
[31] Bhat, R. B., " Natural frequencies of rectangular plates using characteristic orthogonal polynomials in rayleigh-ritz method," Journal of Sound and Vibration, Vol. 102, pp. 493-499, 1985.
[32] Lam, K. Y., and Hung, K. C., "Vibration study on plates with stiffened openings using orthogonal polynomials and partitioning method," Computers & Structures, Vol. 37, pp. 295-301, 1990.
[33] Liew, K. M., Ng, T. Y., and Kitipornchai, S., "A semi-analytical solution for vibration of rectangular plates with abrupt thickness variation," International Journal of Solids and Structures, Vol. 38, pp. 4937-4954, 2001.
[34] Shams, S., and Soltani, B., "Buckling of Laminated Carbon Nanotube-Reinforced Composite Plates on Elastic Foundations Using a Meshfree Method," Arabian Journal for Science and Engineering, Vol. 41, pp. 1981-1993, 2016.
[35] Pradhan, S. C., and Murmu, T., "Small scale effect on the buckling of single-layered graphene sheets under biaxial compression via nonlocal continuum mechanics," Computational Materials Science, Vol. 47, pp. 268-274, 2009.